Insect Inspired Behaviours for the Autonomous Control of Mobile Robots

K. Weber[1], S. Venkatesh[1] and M.V. Srinivasan[2]

[1]Department of Computer Science, Curtin University of Technology, GPO Box U 1987 Perth 6001, Australia. *Email: weberk, svetha@cs.curtin.edu.au*

[2]Centre for Visual Sciences, Research School of Biological Sciences, Australian National University, P.O. Box 475 Canberra, A.C.T. 2601, Australia. *Email: srini@rsbs-central.anu.edu.au*

Abstract

Animals navigate through various uncontrolled environments with seemingly little effort. Flying insects, especially, are quite adept at manoeuvring in complex, unpredictable and possibly hostile environments.

Through both simulation and real-world experiments, we demonstrate the feasibility of equipping a mobile robot with the ability to navigate a corridor environment, in real time, using principles based on insect-based visual guidance. In particular we have used the bees' navigational strategy of measuring object range in terms of image velocity. We have also shown the viability and usefulness of various other insect behaviours: (i) keeping walls equidistant, (ii) slowing down when approaching an object, (iii) regulating speed according to tunnel width, and (iv) using visual motion as a measure of distance travelled.

1 Introduction

Approaches to autonomous robot navigation employing passive vision are attractive in that visual sensors constitute a rich, yet relatively cheap source of information about the surrounding 3D environment. However, visual sensors are also the ones that entail the most computation. Consequently, there is a strong motivation to explore techniques that make simple, qualitative observations of the important properties of a scene.

One way in which to tackle this problem is to examine how relatively simple animals, such as insects, overcome the problems of autonomous navigation. Given their small size and relatively simple nervous systems, it seems likely that insects employ "short cuts" to navigate in the real world. It is these principles that may be applied advantageously to robot navigation. Recent investigations are now showing what sort of visual cues flying insects use to achieve their navigational prowess [3,7,8,15].

2 Background

2.1 Measuring range via apparent motion

Considerable evidence now suggests that moving insects are able to infer the ranges of objects from the apparent motion of their images across the eye [2,9,13,15].

The range (r) of an object can be inferred from its apparent angular velocity (ω), its bearing (θ), and the linear velocity (v) of the eye [11] (see figure 1).

$$r = \left(\frac{v}{\omega}\right) \sin(\theta) \qquad (2.1)$$

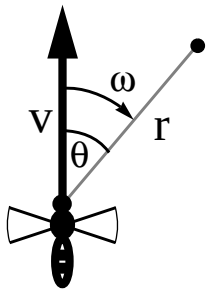

Figure 1 - Range from apparent velocity

2.2 Insect Behaviour

We consider the following subset of insect behaviour as a basis for the development of robust algorithms for corridor traversal.

(i) Peering: before jumping, a locust will sway its head and body laterally to estimate the range of a nearby target in terms of the motion of its image on the retina [13,18].

(ii) Trying to keep obstacles or walls equidistant: it has been shown [15] that honeybees centre their flight paths between obstacles by balancing the speeds of image motion on their two eyes.

(iii) Responding to looming by slowing down: one of the most important flight manoeuvres flying insects

perform is that of landing [1,17].

(iv) Keeping motion speed constant: honeybees have been shown [16] to regulate flight speed by monitoring the speed of apparent motion. Essentially, they strive to hold apparent image speed constant.

(v) Utilizing observed motion as a measure of distance travelled: recent experiments [16] have revealed that honeybees measure distances to goals through the integration of apparent-motion speeds observed en route.

3 Copying Bee Behaviour

Inspired by the way honeybees use apparent motion in their visual navigation, we have attempted to use the same simple cues to provide a mobile robot with the ability to successfully navigate along a corridor environment.

Several similar investigations [4,5,6,12], also inspired by the navigational behaviour of honeybees, have been carried out.

3.1 Improvements upon Previous Approaches

To combat some of the deficiencies of earlier approaches we have implemented and tested the following improvements:

1. In a simple way, the system takes robot rotation into account when calculating range. The effects of rotation on the image motion must be discounted before equation 2.1 can be applied to gauge range. The rotation and translation of the robot are calculated by monitoring wheel speeds. This method avoids the need for active gaze stabilization.

2. An image interpolation method [10,14] is used to calculate apparent motion. The advantages of this technique over previous methods are that there is no need for (i) feature identification/tracking, (ii) measurement of high-order spatial or temporal derivatives, or (iii) iterative calculation. Furthermore, unlike earlier approaches, this technique delivers both slope and range of a surface.

3. Lateral images are used to measure not only the distances to the two side walls, but also their orientation.

4. We present a “virtual motion” strategy for detecting obstacles in the forward direction. Two frontal views are captured along parallel axes that are laterally displaced by a known distance. By measuring the apparent motion between the two images, it is possible to compute the range of the frontal surface. This strategy is analogous in many ways to the sideways “peering” head movements of locusts (see section 2.2). Furthermore, the two frontal images can provide orientation information which can be used to determine the nature of an oncoming obstacle and to control preparatory manoeuvres accordingly.

5. Further, we demonstrate three additional insect behaviours (section 5).

4 Proposed Paradigm

4.1 Simulation

The basis of the simulation is the modelling of the robot’s motion and the analysis of the images acquired from various camera views. Raytracing is used to provide the images that would be seen by the cameras.

The simulated robot is based upon the real mobile robot (section 4.4) which was used for real-world experiments. In simulation, each camera has a 30 degree field of view and provides both frontal and lateral views (figure 2(a)).

4.3 Course Correction

The course correction strategy uses both the range and slope of the walls in determining correct robot heading (figure 2(b)). The tunnel axis (dotted arrow) is defined as the line positioned halfway along the width of the tunnel (the mean of the distances r1 and r2) and oriented in a direction corresponding to mean wall slope. The control rule used makes the robot head for a point that is a specified distance away on the tunnel axis. By altering this distance, the rapidity of the control action can be varied. This strategy ensures that the robot tends towards the corridor centre and then strives to maintain its position.

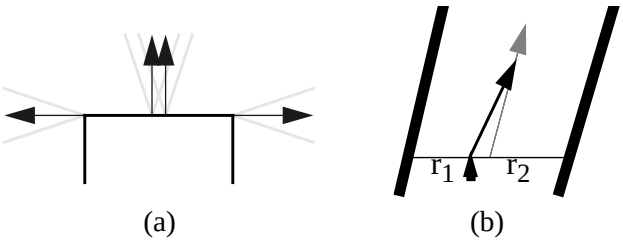

Figure 2 - (a) Robot views; (b) Course Correction

4.4 Real-World Robot Setup and Optics

The mobile robot is tethered to a workstation. It moves on three wheels, consisting of two drive wheels at the front and a trailing castor at the rear (figures 3(a, c, d)). The drive wheels are independently controllable, allowing the robot to move along a curve or even spin on the spot. The robot’s wheel base is 26 cm wide. Maximum manoeuvring speed is approximately 12 cm/s.

The vision for the robot is provided by a miniature CCD video camera, which is placed looking upwards at a mirror assembly (figures 3(a, c)). The mirror assembly directs two lateral and two straight-ahead views onto the imaging plane of the camera. A single camera is used to capture all four views, thus avoiding difficulties associated with balancing automatic gain control systems of multiple cameras. An example image showing the mapping of the

two lateral and two frontal views is shown in figure 3(b).

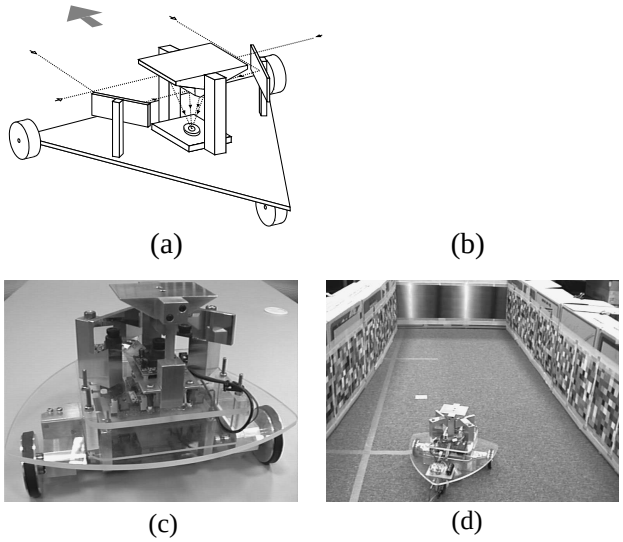

(a) (b)

(c) (d)

Figure 3 - Robot and environment

5 Results

A variety of visually-mediated insect behaviours have been implemented: (i) keeping walls equidistant, (ii) slowing down when approaching an object, (iii) keeping apparent-motion speed constant by altering robot speed, and (iv) integrating visual motion as a measure of distance travelled.

5.1 Keeping walls equidistant

This centring strategy is the basis of the robot's control. Figure 4 shows several sets of results obtained from real-world experiments. The robot's leading edge (wheel base) is shown as it travels up the corridor. The robot moved at an average speed of approximately 10 cm/s.

(a) (b) (c) (d)

Figure 4 - Centring Behaviour (real-world)

5.2 Slowing down due to frontal obstruction

Figure 5(a) shows the simulated robot as it approaches a dead-end passage. Since the motion of the robot is shown by incremental positions of equal temporal spacing, the relative speed of the robot can be seen by the spatial separation. Figures 5(b-d) show the same behaviour for the real robot. Due to the physical limitations of robot speed, the act of slowing down is not clearly visible in figures 5(b-d). The robot is essentially still moving at its top speed when the frontal object is perceived to be too close for comfort and it responds by stopping and spinning.

(a) (b) (c) (d)

Figure 5 - Slowing down for frontal obstacles (a) simulation; (b-d) real-world

5.2.1 Turning a sharp corner by spinning. When the robot gets itself into a very tight situation where normal manoeuvring is unsafe it must make use of a different manoeuvre to extricate itself, which we have implemented as a spinning manoeuvre (as seen in section 5.2).

The spinning behaviour is simply triggered when a frontal obstacle is dangerously close. The robot then stops, and spins on the spot until the frontal range becomes large enough again to resume forward motion (figure 6).

(a) (b) (c)

Figure 6 - Spinning to aid sharp cornering (a) simulation; (b, c) real-world

5.3 Keeping motion speed constant

Figures 7(a, b) show the simulated robot exploring an environment whilst striving to keep the observed (maximum) motion speed constant. This is very useful in that it forces the robot to slow down in tight situations such as where the walls of a corridor become quite narrow.

The robot behaviour in figures 7(a, b) show one of the problems with the purely reactive centring behaviour. The large open spaces tend to "distract" the robot. A wall-following behaviour should probably be employed here. Another possibility is to utilize frontal range information to offset the attraction of large lateral open spaces.

Figures 7(c, d) show the real-world results. In trying to maintain a constant maximum amount of apparent motion, the robot is clearly seen to change its speed. Robot speed varies from 4-12 cm/s approximately.

(a) (b) (c) (d)

Figure 7 - Maintaining constant apparent-motion (a, b) simulation; (c, d) real-world

5.4 Wall following

As was seen in the previous section, there is a clear need for a wall-following behaviour. This is implemented in essentially the same way as the centring behaviour, except that in this case only the information from one side is utilized. The robot strives to maintains a pre-specified distance away from the followed wall. The corridor width is used as the trigger to instigate wall following.

Figures 8(a, b) show how the wall-following behaviour works in the environment that caused problems in figures 7(a, b). Figures 8(c, d) show real-world results without wall-following and in comparison figures 8(e, f) show the robot behaviour with wall-following. Without wall-following the robot heads straight for the open space.

(a) (b) (c) (d) (e) (f)

Figure 8 - With/Without wall-following (a, b) simulation; (c-f) real-world

5.5 Using Image Motion as a Measure of Distance

As suggested in section 2.2 integrated optic flow can provide a viable alternative measure of distance travelled. This alternate measure can be very useful when wheel-based odometry fails or is inappropriate. The integrated optic flow as observed in our results, is the summation of pixel displacements of the left and right fields of view when the robot is in forward motion.

Due to the fact that integrated flow as a measure of distance travelled, is dependent on the environment we have analysed the similarity of these measurements over several runs within a constant environment. We would expect that the natural variation between runs will be cancelled out somewhat by the nature of the integration process. The distances traversed due to the side to side meandering of the robot, for example, would not be integrated into the calculation, thus resulting in a fairly constant average optical flow, which is more representative of pure forward motion.

Figure 9 shows a few simple (simulation) runs, over a straight 5m section of corridor and table 1 shows the results of integrating the optic flow. Figures 9(a, b) show the robot moving at about 20 cm/s whereas figures 9(c, d) show it moving at approximately 40 cm/s.

(a) (b) (c) (d)

Figure 9 - Integrating optic flow (simulation)

There is a noticeable difference between the integrated flow values (*Flow1* in table 1) for the straight paths (a, c) and the centring paths (b, d). *Flow1* is calculated as $Flow1 = \Sigma\ (\omega_L + \omega_R)$. This is primarily caused by the fact that as one moves closer to one of the side walls, the optic flow from that side does not increase at the same rate as the other side decreases. The optic flow of the side being approached increases faster than the flow on the other side decreases. The result is an overall increase in integrated optic flow.

Table 1: Integrated optic flow from figure 9

	speed (cm/s)	total distance (cm)	*Flow1*	*Flow2*
(a)	20	500.5	9509.5	9509.4
(b)	20	508.6	9955.8	9508.5
(c)	40	501.2	9530.8	9530.8
(d)	40	507.9	10101.5	9502.5

An alternative strategy would be to integrate the reciprocal of the flow (*Flow2* in table 1). (In essence integrate range). *Flow2* is calculated as $Flow2 = \Sigma\ 4/(1/\omega_L + 1/\omega_R)$. Since the sum of the ranges to the left and right walls is independent of the robot's position, this strategy should produce a result that does not depend upon the specific trajectory taken by the robot. As can be seen in table 1, *Flow2* does indeed give a more consistent measure of distance.

A batch of real-world experiments, a subset of which is shown in figure 10, has also been conducted and analysed.

These experiments show the behaviour of the real robot traversing the same piece of corridor repeatedly. In experiments (a-g) the robot consistently starts in the centre of the corridor and performs its standard centring behaviour while maintaining an average velocity of approximately 10 cm/s. Experiments (h-m) show the same robot behaviour while maintaining a slower speed of 7.5 cm/s. Finally, the group of experiments (n-w) show the robot behaviour when started off-centre together with variable speed; speed varies between approximately 4 cm/s at the beginning and 12 cm/s after centring has occurred.

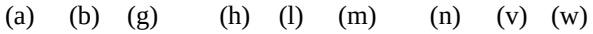

Figure 10 - Subset of real-world experiments

As expected, table 2 shows that integrated optic-flow does indeed correlate well with physical displacement. Also from table 2 it can be seen that *Flow2* does provide a slightly better, more consistent, measure than *Flow1*.

Table 2: *Flow1* (and *Flow2*) statistics for Figure 10

	min.	max.	mean	std. dev.	std. dev. as % of mean
(a)-(g)	23.76 (20.72)	25.50 (21.49)	24.47 (21.29)	0.53 (0.25)	2.17 (1.18)
(h)-(m)	25.04 (20.17)	28.55 (22.41)	26.26 (21.20)	1.28 (0.90)	4.89 (4.23)
(n)-(w)	23.84 (22.01)	25.82 (23.07)	24.74 (22.41)	0.48 (0.32)	1.94 (1.42)
(a)-(w)	23.76 (20.17)	28.55 (23.07)	25.05 (21.76)	1.07 (0.78)	4.27 (3.59)

6 Conclusions

It has been shown that very simple motion cues and behaviours, inspired by the visual navigation of flying insects, can be used profitably to provide a mobile robot with the ability to traverse a corridor environment in real-time. Please see [19] for a more detailed presentation.

In particular we have shown the viability and usefulness of various insect behaviours: (i) utilizing apparent motion to gauge range, (ii) keeping walls equidistant, (iii) slowing down when approaching an object (iv) regulating speed according to tunnel width, and (v) using visual motion as a measure of distance travelled.

7 References

[1] Borst, A. and S. Bahde (1988) Visual information processing in the fly's landing system. J. of Comp. Physiol. A 163: 167-173.
[2] Collett, T.S. and L.I.K. Harkness (1982) Depth vision in animals. In: Analysis of Visual Behaviour (D.J. Ingle, M.A. Goodale and R.J.W. Mansfield eds.), pp. 111-176. M.I.T. Press: Cambridge (Ma).
[3] Collett, T., H-O Nalbach and H. Wagner (1993) Visual stabilisation in arthropods. In: Visual Motion and its Role in the Stabilisation of Gaze (F.A. Miles and J. Wallman eds.), pp. 239-263. Elsevier Science Publishers B.V.: New York.
[4] Coombs, D., M. Herman, T. Hong and M. Nashman (1995) Real-time obstacle avoidance using central divergence and peripheral flow. Proceedings ICCV.
[5] Coombs, D. and K. Roberts (1993) Centering behavior using peripheral vision. Proceedings CVPR, pp. 440-445.
[6] Duchon, A.P. and W.H. Warren (1994) Robot navigation from a Gibsonian viewpoint. Proceedings, IEEE Conference on Systems, Man and Cybernetics, San Antonio, Texas, pp. 2272-7.
[7] Heisenberg, M. and R. Wolf (1993) The sensory-motor link in motion-dependent flight control in flies. In: Visual Motion and its Role in the Stabilization of Gaze (F.A. Miles and J. Wallman eds.), pp. 265-283. Elsevier Science Publishers B.V.: New York.
[8] Hengstenberg, R. (1993) Multisensory control in insect oculomotor systems. In: Visual Motion and its Role in the Stabilization of Gaze (F.A. Miles and J. Wallman eds.), pp. 285-298. Elsevier Science Publishers B.V.: New York.
[9] Horridge, G.A. (1986) A theory of insect vision: velocity parallax. Proc. of the Royal Society of London B 229: 13-27.
[10] Nagle, M.G. and M.V. Srinivasan (1996) Structure from motion: determining the range and orientation of surfaces by image interpolation. J. Opt. Soc. Am. A 13: 25-34.
[11] Nakayama, K. and J.M. Loomis (1974) Optical velocity patterns, velocity-sensitive neurons, and space perception: a hypothesis. Perception 3: 63-80.
[12] Santos-Victor, J., G. Sandini, F. Curotto, and S. Garibaldi (1993) Divergent Stereo for Robot Navigation: Learning from Bees. Proceedings CVPR, pp. 434-439.
[13] Sobel, E.C. (1990) The locust's use of motion parallax to estimate distance. J. Comp. Physiol. A. 167, 579-588.
[14] Srinivasan, M.V. (1994) An Image-interpolation Technique for the Computation of Optic Flow and Egomotion. Biological Cybernetics, 71: 401-415.
[15] Srinivasan, M.V., M. Lehrer, W.H. Kirchner and S.W. Zhang (1991) Range perception through apparent image speed in freely-flying honeybees. Vis. Neurosci. 6: 519-535.
[16] Srinivasan, M.V., S.W. Zhang, M. Lehrer and T.S. Collett (1996) Honeybee navigation en route to the goal: Visual flight control and odometry. J. of Exp. Biol. 199: 155-162.
[17] Wagner, H. (1982) Flow-field variables trigger landing in flies. Nature 297: 147-148.
[18] Wallace, G.K. (1959) Visual scanning in the desert locust Schistocerca gregaria, Forskal. J. Exp. Biol. 36: 512-525.
[19] Weber, K., S. Venkatesh and M.V. Srinivasan (1996) Insect inspired behaviours for the autonomous control of mobile robots. In: From Living Eyes to Seeing Machines (M.V. Srinivasan and S. Venkatesh eds.). Oxford University Press. To appear.